American Journal of Botany 96(9): 1703–1711. 2009.

POLLEN CLUMPING AND WIND DISPERSAL IN AN INVASIVE ANGIOSPERM[1]

MICHAEL D. MARTIN,[2] MARCELO CHAMECKI,[3] GRACE S. BRUSH,[2,6] CHARLES MENEVEAU,[4] AND MARC B. PARLANGE[5]

[2]Department of Geography and Environmental Engineering, Ames Hall, 3400 N. Charles Street, Johns Hopkins University, Baltimore, Maryland 21218 USA; [3]Department of Meteorology, 503 Walker Building, Pennsylvania State University, University Park, Pennsylvania 16802 USA; [4]Department of Mechanical Engineering, Latrobe Hall, 3400 N. Charles Street, Johns Hopkins University, Baltimore, Maryland 21218 USA; and [5]School of Architecture, Civil, and Environmental Engineering, École Polytechnique Fédérale de Lausanne, CH-1015 Lausanne, Switzerland

Pollen dispersal is a fundamental aspect of plant reproductive biology that maintains connectivity between spatially separated populations. Pollen clumping, a characteristic feature of insect-pollinated plants, is generally assumed to be a detriment to wind pollination because clumps disperse shorter distances than do solitary pollen grains. Yet pollen clumps have been observed in dispersion studies of some widely distributed wind-pollinated species. We used *Ambrosia artemisiifolia* (common ragweed; Asteraceae), a successful invasive angiosperm, to investigate the effect of clumping on wind dispersal of pollen under natural conditions in a large field. Results of simultaneous measurements of clump size both in pollen shedding from male flowers and airborne pollen being dispersed in the atmosphere are combined with a transport model to show that rather than being detrimental, clumps may actually be advantageous for wind pollination. Initial clumps can pollinate the parent population, while smaller clumps that arise from breakup of larger clumps can cross-pollinate distant populations.

Key words: *Ambrosia artemisiifolia*; anemophily; Asteraceae; cross-pollination; genetic diversity; pollen clumps; pollen dispersal; wind pollination.

Effective pollen dispersal between plant populations is vital for maintenance of genetic diversity (Sork and Smouse, 2006; Nakanishi et al., 2009). A thorough understanding of pollen dispersal dynamics is necessary for accurately modeling long-distance dispersal of plant genes (Nathan, 2006), managing pollination contamination between populations (Dow and Ashley, 1998), and conserving threatened plant populations in the face of habitat fragmentation and global climate change (Knapp et al., 2001; Hamrick, 2004; O'Connell et al., 2006). In general, pollen is dispersed either by wind or by animals, mainly insects. However, insects are known to visit some wind-pollinated plants, and wind is known to disperse pollen from some insect-pollinated plants, which greatly complicates the issue and suggests a continuum of pollination syndromes, especially for species in transition from one syndrome to another (Culley et al., 2002). Although anemophily (wind pollination) is the norm for gymnosperms, entomophily (insect pollination) is the primitive condition in angiosperms (Whitehead, 1969). Anemophily is found in 16% of angiosperm families, the result of more than 60 independent evolutions from insect- or animal-pollinated ancestors (Linder, 1998).

In most anemophilous species, pollen is dispersed as single grains, whereas in entomophilous plants, pollen emerges from the anther in clumps (Faegri and van der Pijl, 1966; Hesse, 1981; Ackerman, 2000; Harder and Johnson, 2008). Pollen clumping is generally assumed to have negative consequences for wind pollination because clumps have larger settling velocities and so disperse shorter distances than solitary pollen grains (Faegri and van der Pijl, 1966; Tauber, 1977; Niklas and Buchmann, 1988). Despite this theoretical impediment, pollen clumps have been observed in dispersion studies of many common and widely distributed wind-pollinated species (Andersen, 1970; Tonsor, 1985; Niklas and Buchmann, 1988; Di-Giovanni et al., 1995; Lisci et al., 1996).

The genus *Ambrosia* L. (Asteraceae) is an anemophilous plant mostly native to North America, the pollen of which is highly allergenic and, as a result of the presence of pollenkitt, is released in large clumps (Bianchi et al., 1959; Dingle et al., 1959; Payne, 1966; Pacini and Franchi, 1998). Staminate (male) flowers of *A. artemisiifolia* and *A. trifida* (giant ragweed) display a number of features that indicate specialization for wind pollination, including downward release of pollen and position above the pistillate (female) flowers; inconspicuous coloring and size reduction; apical appendages on each of the five anthers, which aid in dehiscence; and the presence of the pistillodium, an organ that extends along the central floral axis during and after anther dehiscence and is believed to assist in removal of pollen from the interior of the flower (Dowding, 1987; Curtis and Lersten, 1995).

Ambrosia artemisiifolia is an unrelenting invasive outside of its native range, and the plant has reached almost the entire Earth over the last few centuries (Wang et al., 1985; Bass et al., 2000; Laaidi et al., 2003; Kiss and Béres, 2006). Pollen preserved in sediment cores from bogs and lakes have shown that for the majority of its postglacial history, except for a short period in the early Holocene, *Ambrosia* has been a relatively uncommon plant (Grimm, 2001; Faison et al., 2006). During this time and just before European settlement, when much of the land was in native forest and grassland, *Ambrosia* probably existed in small, isolated populations along riverbanks or in open

[1] Manuscript received 5 December 2008; revision accepted 13 April 2009.

The authors thank A. Rinaldo, R. Schlaepfer, and two anonymous reviewers for comments on the manuscript and B. DeTemple, C. Higgins, M. Spicknall, M. Embry, L. Ziska, and S. Featherstone for assistance in experimental design and setup. This research was supported by National Science Foundation awards BES-0119903 and EAR-0609690.

[6] Author for correspondence (e-mail: gbrush@jhu.edu)

doi:10.3732/ajb.0800407

forest patches created by tree fall (Wodehouse, 1971). However, once the land was cleared for agriculture, *Ambrosia* invaded open fields, forming dense populations that dominated much of the landscape (Davis, 1976; Abul-Fatih and Bazzaz, 1979; Brush, 1989).

The extremely clumpy nature of *A. artemisiifolia* pollen is paradoxical. On the one hand, large settling velocities should reduce pollen dispersal to very short distances, limiting significant gene flow to local conspecifics and yielding negative consequences like inbreeding and genetic drift (Ghazoul, 2005). On the other hand, airborne *A. artemisiifolia* pollen is commonly dispersed far from any known source population, and its extraordinary success as an invasive indicates that populations are healthy and genetically diverse (Genton et al., 2005; Lorenzo et al., 2006; Stach et al., 2007). *Ambrosia artemisiifoilia* also maintains consistently high outcrossing rates regardless of plant spacing (Friedman and Barrett, 2008). These observations indicate that, at least for *A. artemisiifolia*, genetic detriments resulting from pollen clumping are not significant.

We used a dense, 6-ha stand of *A. artemisiifolia* as a model system to investigate the influence of pollen clumping on wind dispersal of pollen. Our study combines simultaneous measurements of micrometeorological conditions and novel, quantitative methods for measuring clump size in pollen shedding from anemophilous flowers as well as airborne pollen being dispersed by wind above the *A. artemisiifolia* canopy. These measurements are then used in a mathematical model of the turbulent pollen plume downwind of a pollen source to study dispersal of different sizes of pollen clumps. We provide a theoretical framework that suggests clumping may be an advanced dispersal strategy for anemophilous plants with individual spacing distributions similar to *A. artemisiifolia*.

MATERIALS AND METHODS

Field observations—Data were collected during September and October 2006 in a fallow corn field invaded by *Ambrosia artemisiifolia* in Upper Marlboro, Maryland, USA (38°52′42″N 76°46′42″W). The 6-ha, approximately square field had been harvested and mowed in 2005 and was left undisturbed throughout 2006. We divided the field into 1-m^2 plots, randomly choosing 25 plots for a vegetation analysis in which we counted all plants. In 10 of these plots, we also measured the height of each plant. The field was dominated by *A. artemisiifolia*. The average density of mature (height > 20 cm) *A. artemisiifolia* was 89 plants/m^2, yielding an estimated 5.3 million mature plants in the field. The average height of the mature *A. artemisiifolia* plants was 69 ± 30.2 cm (mean ± SD).

We characterized clumping during pollen shed from the staminate flowers using over 70 h of microscale videos that captured the diurnal pollen release at 30 frames/s with a tripod-mounted digital camcorder (DSR-PD170, Sony Electronics, San Diego, California, USA) and a reversed lens. We reduced motion of the inflorescence-bearing *A. artemisiifolia* branch by wiring it to a metal stake. A length scale for the video was provided by placing a ruler with micrometer-scale markings within the camera's field of view. Seven hours of video from a single day (21 September) were analyzed to monitor atmospheric entrainment events from the mass of pollen protruding from a single staminate flower following anther dehiscence. We chose the 21 September video for its image quality and because it captured a relatively large number of pollen entrainment events. Experimental videos from other days showed that pollen release on 21 September was representative of the process in general.

We also collected hourly airborne pollen samples using Rotorod pollen samplers (Multidata, Plymouth Meeting, Pennsylvania, USA) spaced along a single 6-m vertical pole near the east side of the field. (The prevailing wind was from the west.) A 6-m tower for the meteorological equipment was placed 15 m south of the pole. Meteorological data were sampled continuously at 10 Hz using a datalogger (CR-5000, Campbell Scientific, Logan, Utah, USA). We measured wind speed and direction (propeller anemometer 05103; R. M. Young, Traverse City, Michigan, USA) at 6 m, temperature and relative humidity (probes HMP45C, Vaisala, Woburn, Massachusetts, USA) at 3 m and 5 m, and net radiation (Net Radiometer Q7, Radiation and Energy Systems, Seattle, Washington, USA) at 3 m. Turbulent fluxes were measured using the eddy covariance method with two sonic anemometers (CSAT3, Campbell Scientific) and one Krypton Hygrometer (KH20, Campbell Scientific) at 3 m.

Analysis of airborne pollen clumping—We counted *Ambrosia* pollen grains on Rotorod samples under a light microscope and then used the counts to calculate airborne pollen concentrations. We selected one day (15 September) of data for analysis of airborne pollen clumping based on steady and strong eastward wind and high concentrations of airborne pollen. For each Rotorod sample, we took overlapping, microscopic digital images of the entire 1.52 mm × 36 mm collecting surface and then united them into a single image of resolution high enough that the *Ambrosia* pollen could be easily identified by eye. Then, after removing the border regions of each image to eliminate potential effects on pollen capture near the edge of the sampling rod, we used MATLAB Image Processing Toolbox software (version 4.2, The Mathworks, Natick, Massachusetts, USA) to recognize each pollen grain and to identify its center coordinates. This procedure was necessary as we detected nearly 40 000 pollen grains in total. All results from the image analysis with pollen recognition software were then checked for accuracy by human eye. We used these coordinates to calculate the radial density function (RDF), $g(r)$, for each sample.

The RDF is an easily calculable and widely relevant statistical metric that can be used as a tool to objectively quantify the degree of clumping/aggregation of any distribution of objects (Glass and Tobler, 1971; Wang et al., 2000; Younge et al., 2004). In our analysis, the RDF, $g(r)$, of the pollen distribution on a given Rotorod sample can be described as

$$g(r) = \left(\frac{\text{probability of finding a grain at } r}{\text{probability of finding a grain at } r \text{ if uniformly distributed}} \right), \quad (1)$$

where r is the distance from the center of a random pollen grain. This function is equivalent to a probability density function of center-to-center distances between grains normalized by the probability density function for a uniform distribution of an equivalent number of grains. A measured value of $g(r) = 1$ indicates that the experimental distribution is uniform at that value of r. The numerator of Eq. 1 is calculated as the ensemble average (over all grains) of the fraction of total grains at a distance r from each grain. The denominator of Eq. 1 is calculated with the same measurement as in the numerator, but with a model distribution of an equal number of pollen grain whose positions are randomly distributed on a rectangular area equal to that of the Rotorod sample. The pollen grain positions are randomly distributed except that the grains are "hard-shelled" and thus are not allowed to overlap; if two grains overlap, one is slightly nudged so that the center-to-center distance is $d = 20$ μm. Younge et al. (2004) provides an excellent description of the calculation of $g(r)$ in a different system of hard-shelled spheres.

→

Fig. 1. Video frames showing clump size measurement and wind erosion of pollen mass for *Ambrosia artemisiifolia*. (A) At 0850 hours, pollen mass protrudes from corolla lobes. (B) Frame immediately following the frame in (A). Pink contour indicates projected border (silhouette) of pollen mass from (A). Green circles of maximum possible diameter (d_{clump}) were fit within the borders of the silhouettes from the two consecutive video frames. (C) At 0851 hours, rapidly eroding pollen mass. Pink contour indicates the pollen mass silhouette from (B). (D) At 1153 hours, pollen mass mostly eroded, revealing extended anther claws. Pink contour indicates silhouette of pollen mass from (C). Black arrow indicates the extending pistillodium. (E) At 1448 hours, the pistillodium extension pushes remaining pollen away from flower. Blue contour indicates the silhouette of the remaining pollen mass, which is now entirely visible. (F) At 1503 hours, pollen mass has completely eroded from pistillodium's trichomes.

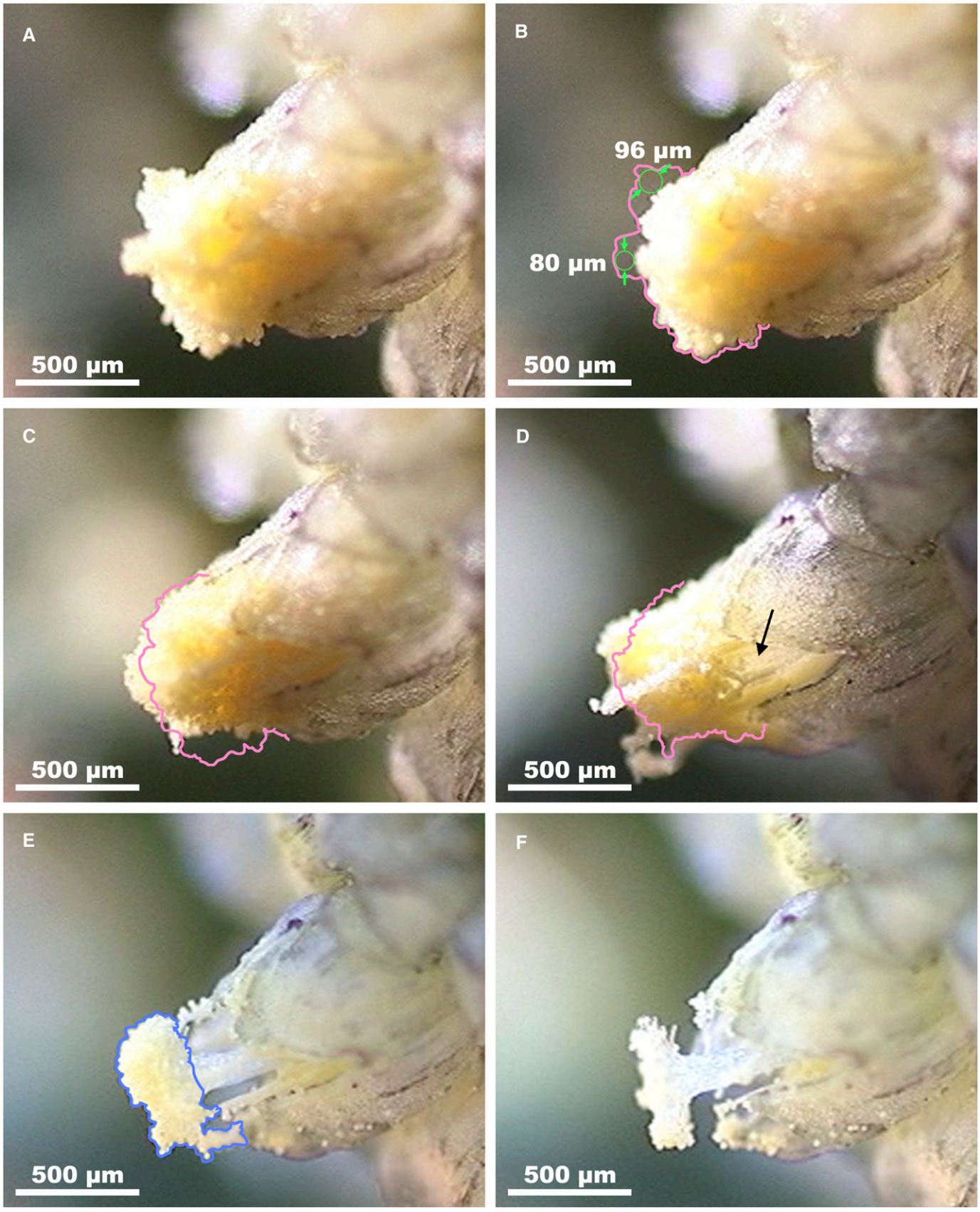
A
500 µm
B
96 µm
80 µm
500 µm
C
500 µm
D
500 µm
E
500 µm
F
500 µm

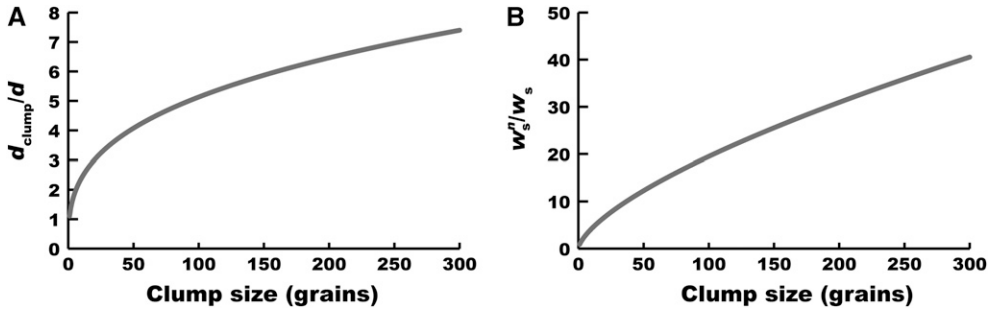

Fig. 2. Theoretical characteristics of idealized spherical pollen clumps. (A) The diameter (d_{clump}) of a spherical clump (normalized by average pollen grain diameter d) as a function of the number of clumped grains n. (B) The ideal settling velocity w_s^n (normalized by empirically determined settling velocity w_s of a single pollen grain) as a function of the number of clumped pollen grains n.

Analysis of shed pollen clumping—We superimposed consecutive video frames captured immediately before and after atmospheric entrainment events to locate a void of pollen in the silhouettes of the pollen mass against a neutral background. The largest possible circle was fit within the boundary of the two silhouettes, and the diameter of this circle was measured (Fig. 1A, B). We used an ideal spherical clumps model to estimate the number of pollen grains contained within a sphere with a diameter equal to that of the best-fit circle. In the model, clumps are assumed to be spherical and optimally packed so that the spherical clump contains the largest number of spherical pollen grains that can possibly fit within its volume. The maximum possible packing density η_{max} was suggested by Kepler in 1611 to be $\eta_{max} = \pi/\sqrt{18}$ (Kepler, 2009). The total volume occupied by pollen in each clump V_{pollen} is equal to the number of grains n times the volume of a grain $\pi d^3/6$, where d is the diameter of a grain. Therefore, the volume of the clump V_{clump} containing n grains is given by $V_{clump} = V_{pollen}/\eta_{max}$, and the diameter of the clump is $d_{clump} = (n/\eta_{max})^{\frac{1}{3}} d$. We assumed the remaining volume between the pollen grains to be filled by air, so the density of the idealized spherical clump is $\rho_{clump} = \eta_{max}\rho_p + (1-\eta_{max})\rho_f$, where ρ_p is the pollen density and ρ_f is the density of the air filling the space between pollen grains. The equivalent diameter of the clump d_{clump} normalized by the average *A. artemisiifolia* pollen diameter d is plotted as function of the number of clumped grains in Fig. 2A.

Model of pollen dispersal—The transport of pollen and seeds by turbulent wind is a field of active research with implications for maintenance of gene flow between isolated populations and for colonization of remote locales (Okubo and Levin, 1989; Nathan et al., 2002). This is a complex problem because dispersal will depend on the relative importance of sedimentation due to gravity (represented by the settling velocity), turbulent diffusion, and transport by the mean wind velocity (Chamecki et al., 2007). To investigate differences in turbulent dispersal of clumped and unclumped pollen, we developed a mathematical model that predicts the two-dimensional (2-D) average plume of pollen vs. elevation (z) and distance downwind (x) of a source emitting pollen clumps of various sizes. The final equation gives the average, 2-D pollen concentration distribution as a function of a number of environmental factors for which we obtained values through common assumptions and measurement with equipment deployed in the field. A more detailed description of the mathematical model follows.

In the mathematical model, individual clumps are not represented discretely. Instead, we assumed a continuous airborne pollen clump concentration field C. Conservation of pollen mass was mathematically represented by the advection–diffusion equation that includes a gravitational settling term (e.g., see Pasquill and Smith (1983)). For simplicity, we used a 2-D version of the problem where only the downwind and vertical directions (x and z) were considered. This can be interpreted as a planar cross-section through a 3-D line source or as an approximation of the cross-wind integrated solution of a three-dimensional point source (Godson, 1957).

Because we are not interested in the transient details of the instantaneous plume, the Reynolds-averaged, steady-state version of the advection–diffusion equation is applied:

$$U(z)\frac{\partial \bar{C}(x,z)}{\partial x} = \frac{\partial}{\partial z}\left(K_c(z)\frac{\partial \bar{C}(x,z)}{\partial x} + w_s\bar{C}(x,z)\right). \quad (2)$$

In Eq. 2, $U(z)$ is the average wind speed profile, $\bar{C}(x,z)$ is the average concentration plume (in grains/m^2), $K_c(z)$ is the eddy-diffusivity of pollen concentration (a measure of the efficiency of the turbulence in dispersing pollen grains), and w_s is the settling velocity of pollen particles.

Under neutral stability conditions in the atmospheric boundary layer, the vertical profiles of wind speed can be approximated by the power law

$$U(z) = qu_*\left(\frac{z}{z_0}\right)^{\alpha}, \quad (3)$$

where q and α are constants to be determined, u_* is the friction velocity, and z_0 is the surface roughness length scale. Under the same conditions, the eddy-diffusivity is often assumed to be $K_c = \kappa z u_*$ (Kaimal and Finnigan, 1994), κ = 0.4 being the von Kármán constant. Using these profiles, an analytical solution to Eq. (2) for a point source at height $z = h$ emitting at a rate Q can be obtained (Rounds, 1955):

$$\frac{\bar{C}(x,z)}{Q} = \frac{A}{x}\frac{\gamma}{hU(h)}\left(\frac{z}{h}\right)^{-\left(\frac{\gamma p}{2}\right)}\exp\left(-\frac{A}{x}\left[1+\left(\frac{z}{h}\right)^{\gamma}\right]\right)I_p\left\{\frac{2A}{x}\left(\frac{z}{h}\right)^{\frac{\gamma}{2}}\right\}, \quad (4)$$

where I_p is the modified Bessel function of the first kind of order p, $\gamma = 1 + \alpha$, and

$$A = \frac{hU(h)}{\gamma^2\kappa u_*}, \qquad \alpha = \frac{\log\left(\frac{z_0}{h}\right)}{1+\log\left(\frac{z_0}{h}\right)} - 1, \qquad p = \frac{w_s}{\gamma\kappa u_*}. \quad (5)$$

Eq. 4 describes the dispersion of solitary pollen grains and pollen clumps as well, if the appropriate settling velocity is used. Usually the settling velocity of small particles is assumed to be equal to the terminal velocity in still fluid, which is determined by Stokes' law assuming a spherical particle:

$$w_s = \frac{(\rho_p - \rho_f)gd^2}{18\mu}, \quad (6)$$

where g is the acceleration due to gravity, d is the diameter of the particle, and μ is the dynamic viscosity of the fluid. For *A. artemisiifolia* pollen grains, the usual values are d = 20 μm and w_s = 0.0156 m/s (Raynor et al., 1970).

Assuming that the clumps are spherical, the expressions for clump diameter and density from the previous section can be used to obtain an expression for settling velocity of a clump containing n grains:

$$w_s^n = (n^2\eta_{max})^{\frac{1}{3}}\frac{(\rho_p - \rho_f)gd^2}{18\mu} = (n^2\eta_{max})^{\frac{1}{3}}w_s. \quad (7)$$

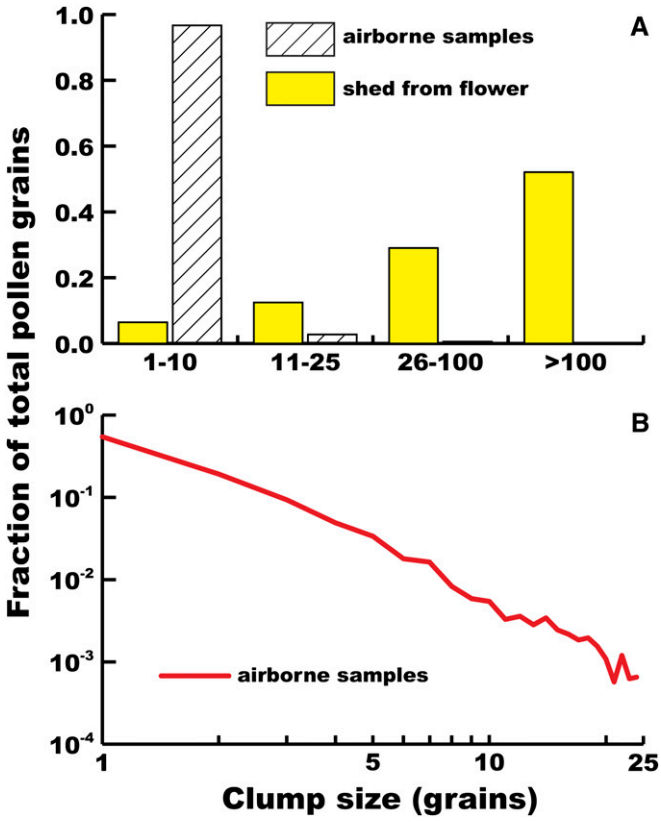

Fig. 3. Size distribution of clumps shed from the flower and those captured in airborne samples of *Ambrosia artemisiifolia*. (A) Distribution of clump sizes for shed pollen and airborne pollen. The largest clump observed during pollen shed from the floret contained 264 grains. (B) Distribution of airborne clump sizes on a logarithmic scale. Although not representative of typical airborne pollen clump size, the largest clumps identified from all the Rotorod samples, one of each size, were 26, 27, 29, 30, 38, and 64 grains.

The settling velocity of clumps is plotted as a function of the number of grains n in Fig. 2B.

We used the solution to Eq. 4 to obtain the fraction of the emitted pollen grains being advected through the region of the pistillate flowers at a given distance from the source. Assuming that the pistillate flowers are localized in the vertical range $h_{inf} \le z \le h_{sup}$, where h_{sup} is the the ground elevation and h_{inf} is the average *A. artemisiifolia* plant height, the total normalized flux of pollen grains through this interval is

$$F(z) = \int_{h_{inf}}^{h_{sup}} \frac{\bar{C}(x,z)}{Q} U(z)dz. \quad (8)$$

RESULTS AND DISCUSSION

General observation of the pollen release videos indicates that the atmospheric entrainment of pollen from staminate flowers of *A. artemisiifolia* is characterized by a process of break-off and wind erosion of pollen protruding from the floral interior. Shortly after anther dehiscence, a mass of fresh pollen fills the floral cavity and begins to protrude from corolla lobes (Fig. 1A). Turbulent morning winds continually erode the outermost layers of pollen and disperse them into the atmosphere (Fig. 1B–F). Entrainment events occur in short bursts during strong gusts of wind (measured by sonic anemometers) that interrupt long periods of inactivity at lower wind velocities. Depicted in Fig. 1A and Fig. 1B are consecutive video frames, separated by an interval of 30 ms, immediately preceding and following two simultaneous entrainment events. Green circles of maximum possible diameter (d_{clump} = 80 μm and d_{clump} = 96 μm) fit within the borders of the silhouettes from the two consecutive video frames indicate that the clumps consist of at least 48 grains and 83 grains, respectively. In Fig. 1D, the pollen mass has undergone major erosion, partially revealing the extending pistillodium and anther claws, which appear to provide a support structure for the pollen (Curtis and Lersten, 1995). Figure 1E shows the pistillodium near maximum extension as it pushes the remaining pollen away from the flower (Curtis and Lersten, 1995). The pollen mass has been completely eroded from the pistillodium's trichomes by midafternoon (Fig. 1F).

The entrainment of large clumps of pollen containing hundreds of grains dominates the pollen shedding process as shown in Fig. 3A, where the fraction of total entrained pollen grains measured is presented for different clump sizes (yellow histogram). The distribution shows that 52% of the pollen grains existed in clumps larger than 100 grains, with the largest clump containing at least 264 grains. Clumps containing less than 11

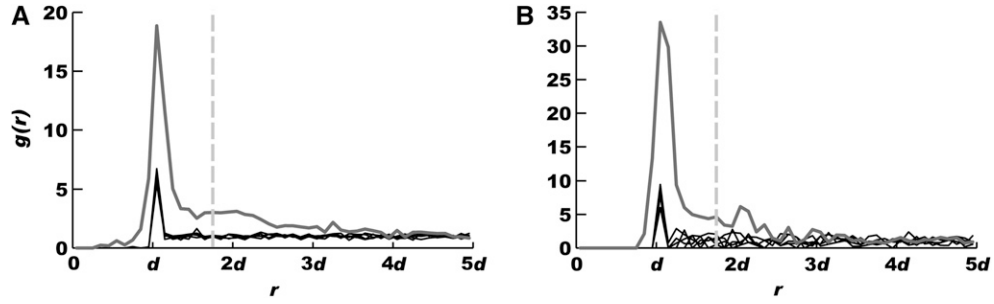

Fig. 4. Radial distribution functions from airborne pollen samples of *Ambrosia artemisiifolia* indicate significant clumping. Gray plots are $g(r)$ data from two representative Rotorod pollen samples. The overlapping black plots are data from five random, approximately uniform pollen distributions with an equivalent number of pollen grains per unit area; d = 20 μm is the average diameter of an *A. artemisiifolia* pollen grain. The dashed line indicates the threshold distance $d_{th} = 1.75d$ chosen to "define" clumps. This distance was chosen because, for the typical Rotorod sample, most of the deviation from the randomized data falls where $r \le 1.75d$. (A) Data from a Rotorod sample taken at 2.4 m elevation over the time interval 1450–1545 hours and with a grain density of 79 grains/mm^2. (B) Data from a Rotorod sample taken at 2.4 m elevation from 1550 to 1645 hours (EDT) and with a grain density of 24 grains/mm^2.

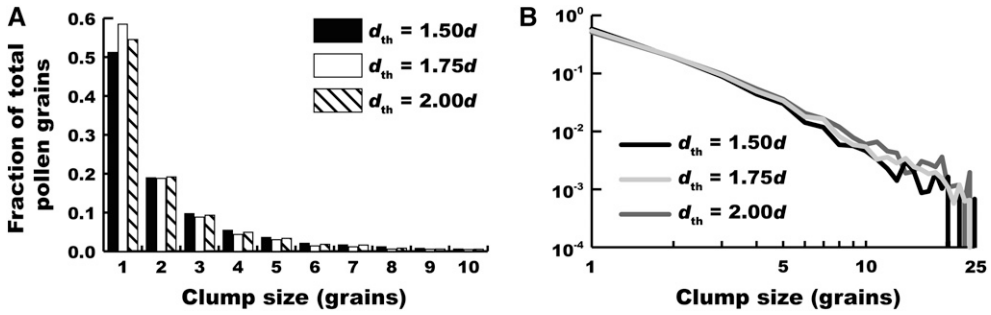

Fig. 5. Effect of value of threshold distance on airborne pollen clumping structure for *Ambrosia artemisiifolia*. Shown are plots of the distribution of clump sizes on the Rotorod pollen samples. Clump size distributions were determined by grouping into a single clump all adjacent pollen grains whose center-to-center distances were less than or equal to d_{th}, a distance chosen subjectively. Each distribution was determined for three different threshold distance d_{th} values and plotted on an (A) arithmetic scale and (B) logarithmic scale. The homogeneity of the clump size distributions shows that our choice of $d_{th} = 1.75d$ is robust.

grains made up only 7% of the estimated total number of pollen grains entrained throughout the day. Although stabilizing the floret by binding the branch may have an effect on the size distribution of shed pollen clumps, we would not expect any significant impact on the main conclusion of this work (that most of the pollen is released in very large clumps). If there were any effect, the flower would be subjected to less movement, which should decrease the size of the clumps that are eroded from the pollen mass.

To investigate differences in clump size distribution of shed pollen and airborne pollen being dispersed above the canopy, we characterized the distribution of pollen grains on Rotorod samples taken at four heights (2.0–6.0 m elevation) during nine 1-h sampling intervals throughout a single day. We then calculated the radial density function (RDF) for each sample. We compared the RDF of each pollen sample to that of five randomly generated distributions of *Ambrosia* pollen grains (modeled as nonoverlapping spheres with $d = 20$ μm, the average grain diameter from our measurements) with the same number of grains per unit area. For grain-to-grain distances between about $0.5d$ and $1.75d$, values of $g(r)$ from our Rotorod samples typically far exceed those of the randomly generated distributions. This indicates that pollen grains on our Rotorod samples are far more "clumpy" than the randomly generated distributions (Fig. 4). The RDFs were also used to "define" pollen clumps on the rods in an objective manner. Considering the entire set of RDFs, we chose a somewhat arbitrary threshold distance $d_{th} = 1.75d$ between clumped pollen grains that ensured that most of the nonrandom part of the each RDF was considered. We used the pollen grain coordinates to calculate the center-to-center distance from each grain to all the other grains in a sample, and grains separated by a distance less than d_{th} were considered a clump. We investigated the sensitivity of d_{th} to our chosen value and found it to be quite robust with very little dependence on the specific value of threshold distance (Fig. 5).

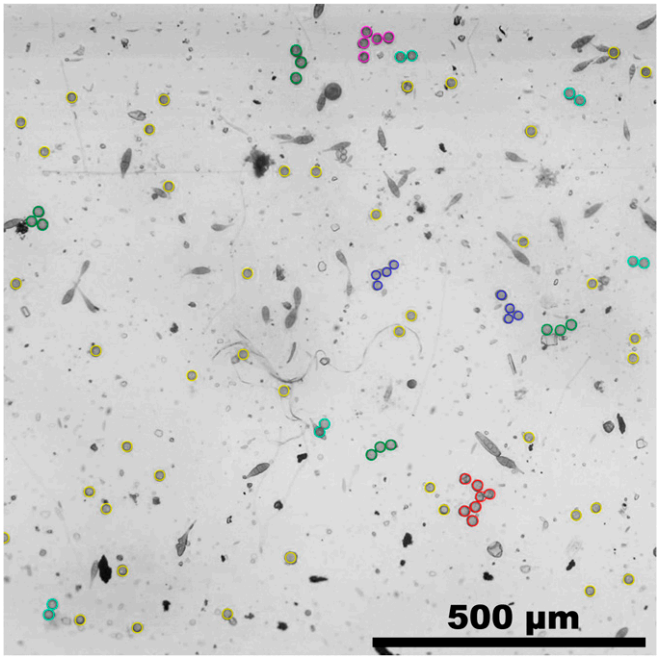

Fig. 6. Pollen clumps of *Ambrosia artemisiifolia* identified within a region of a Rotorod sample. Colored clump outlines overlay a grayscale image depicting less than 3% of the area of a single Rotorod sample's collecting surface. Solitary *Ambrosia* grains are represented by a yellow outline; 2-grain clumps are aquamarine; 3, green; 4, blue; 5, violet; 6 or more, red.

Contrary to our expectations, there is no obvious correlation between the size distribution of the clumps and the elevation or the time of day at which they were sampled. In fact, the number of grains in clumps and the frequency of various clump sizes were remarkably uniform throughout the entire diurnal period of pollen release. Therefore, the results presented here are an average of measurements from 35 individual Rotorod samples. Figure 3B shows the distribution of pollen clump sizes on the Rotorod samples. It is important to note that although the fraction of total pollen decays quickly as clump size increases, the percentage of solitary grains in the airborne pollen is approximately 55%. The remaining 45% are distributed in clumps of different sizes. A small portion of one typical Rotorod sample is shown in Fig. 6.

It is evident that the pollen clumps captured above the canopy were considerably smaller than the clumps shed from the staminate flowers (Fig. 3A). This fact, together with the high frequency of isolated grains in the airborne samples, strongly suggests that once they leave the plant, the large pollen clumps are quickly broken into much smaller clumps by the turbulent wind. Because the large clumps shed from the flower are on the order of the size of the turbulent Kolmogorov scale (the smallest relevant length scales in the flow, typically about 1 mm

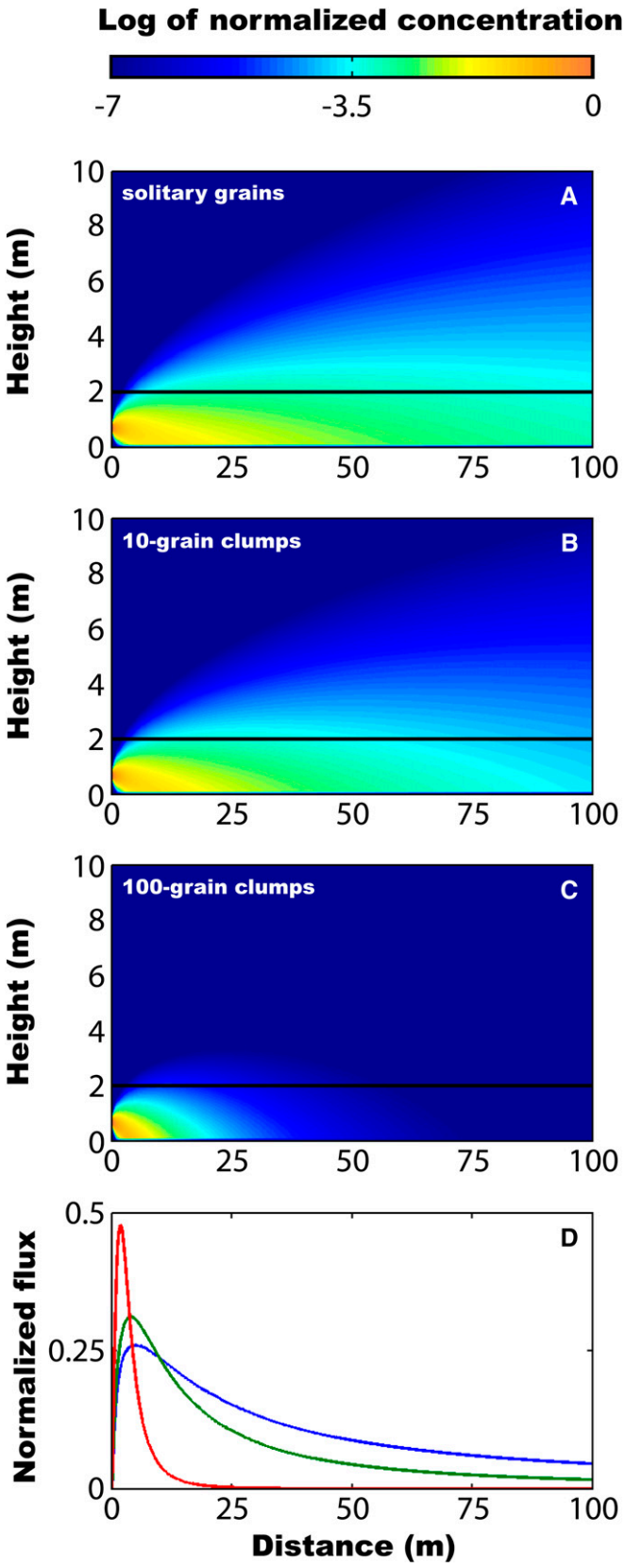

Fig. 7. Theoretical downwind dispersal of pollen clumps. The average pollen clump concentration plume is shown for (A) solitary (unclumped) grains, (B) 10-grain clumps, and (C) 100-grain clumps. The horizontal black line indicates the lowest sampling height in the field observations. (D) Fraction of pollen clumps being dispersed through the region of pistillate flowers as a function of distance from the source plant for different clump sizes. Blue, green, and red curves indicate model predictions for solitary grains, 10-grain clumps, and 100-grain clumps, respectively. Pistillate flowers are assumed to be located between the ground surface and average *Ambrosia artemisiifolia* plant height.

[Pope, 2000]), they are subject to the strongest shear forces in the flow and are more likely to disaggregate. Turbulent breakup of particle aggregates is a well-known, but not well-understood, phenomenon observed in a wide range of fields (Serra et al., 1997; Andersson and Andersson, 2006).

To determine what clump sizes we should expect to find at the elevations of the Rotorod samplers, we used the mathematical model given by Eqs. 4, 5, and 7 to obtain theoretical dispersal plumes for a single plant continuously releasing pollen. The dispersal model relies on our estimations of settling velocity for each clump size. The pollen release height was set at $h = 0.7$ m, the mean height of *A. artemisiifolia* plants in the experimental field, because most of *A. artemisiifolia*'s staminate flowers are located at the top of the plant. The values $u_* = 0.3$ m/s and $z_0 = 0.01$ m were used in the model. These values are characteristic of the measurements recorded by the meteorological instruments during sunlight hours throughout the field study. Although variability in these parameters could have a significant effect on the model, it would affect dispersion of all clump sizes in a similar way. We are not interested in absolute values of dispersion, but rather on comparing dispersion of clumps of different sizes, and the comparative scenario would not be changed.

The resulting clump concentrations are normalized by the source strength and should be interpreted as the average downwind concentration of pollen dispersal units, be they solitary grains or pollen clumps. The results are shown in Fig. 7A–C, in which orange and yellow colors represent high concentrations, and dark blue represents nearly zero concentration. The dispersion plumes for solitary grains and 10-grain clumps are very similar (Fig. 7A, B). The reduced plume for 100-grain clumps stands in contrast to the others, reflecting the larger settling velocities for these large clumps (Fig. 7C). An important point is that although the plume for the 100-grain clumps decays more quickly, it still reaches a height of 2m, the location of the lowest Rotorod airborne pollen sampler. In the field study, no large clumps were observed at the 2 m height. We proposed a clump disaggregation process to explain the major differences in pollen clump size distribution observed during pollen release and in the air above the canopy. That process also explains the discrepancy between our field observations and expectations from the dispersal model; the turbulent wind acts to quickly disaggregate pollen clumps. Therefore, we would not expect to observe them on the Rotorod samples.

Regrettably, pollen clumping complicates our understanding of pollen dispersal from wind-pollinated plants. For example, Tonsor (1985) showed that pollen clumping produces a downwind pattern of gene flow that is not intuitive, because it depends directly on the distribution of the sizes of pollen clumps. We examined the theoretical effect of pollen clumping on the potential for wind pollination using the average dispersal plumes given by the model. From Eq. 8, we calculated the total horizontal flux of pollen dispersal units through the downwind space containing pistillate floral organs, approximated as the

region between pollen emission height (mean plant height) and ground level (Fig. 7D). These curves can be interpreted as the fraction of total pollen dispersal units passing through the zone of potential wind pollination at each distance downwind. Integration of the total flux through the pollination region over all downwind distances yields that solitary grains are, in total, about five times as likely as 100-grain clumps to encounter pistillate flowers. However, it is clear that for the near field, larger clumps are more effective for pollination because a larger fraction of 100-grain clumps passes through the region of pistillate flowers. Considering only downwind distances in the range 0–3 m, 100-grain clumps are nearly twice as effective as solitary grains. The 100-grain clumps are the most effective pollinators in the downwind distance range 0–10 m, while 10-grain clumps are the most effective in the range 10–21 m, and solitary grains are the most effective beyond 21 m. This suggests that particularly for small, dense, isolated populations such as those likely formed by precolonial *A. artemisiifolia*, pollination might be most effectively accomplished by combining a broad range of clump sizes, the larger ones more effective in the near field and the smaller ones in the far field. We propose that this range of clump sizes would be automatically generated through breakdown due to turbulent wind.

This study confirms the observations of previous researchers that the vast majority of *A. artemisiifolia* pollen is initially shed from the staminate flowers in large clumps. However, examination of pollen samples collected at various elevations above the canopy shows that airborne *A. artemisiifolia* pollen exists as a largely homogeneous plume of much smaller clumps, suggesting the following scenario for the dynamics of *A. artemisiifolia* pollen dispersal: Early morning anther dehiscence extrudes a growing mass of fresh pollen from the flower's interior, exposing it to the atmosphere. The forces exerted on the pollen mass by the turbulent wind cause large clumps usually consisting of hundreds of pollen grains to break off and become entrained into the atmosphere. During atmospheric transport, large clumps continuously break into smaller ones due to turbulent wind stresses. Large clumps of pollen like those observed during pollen shedding were rarely observed in pollen samples collected above the canopy, indicating that clump breakdown occurs relatively quickly. Our hypothesis of turbulent disaggregation of pollen clumps explains observations by Player (1979) and Lisci et al. (1996) that pollen clump size tended to be inversely proportional to mean wind velocity; higher wind velocities generate more turbulence in environmental flows, which would more quickly and thoroughly disaggregate pollen clumps. It should be noted that previous researchers describe for the initially released pollen clumps a period of adherence to surrounding vegetation before eventual entrainment into the lower atmosphere (Bianchi et al., 1959). Although collisions with vegetation and possible drying of the clumps may assist the break-up process, there is no evidence that pollen is then entrained as single grains. Even if this description were correct, pollen clump entrainment is still possible, and our model of turbulent break-up is still valid.

Our results contradict the assumption that pollen clumping, usually associated with insect pollination, is necessarily detrimental for wind-pollinated plants such as *A. artemisiifolia*, because atmospheric turbulence rapidly disaggregates large clumps into smaller clumps and solitary grains. The large clumps that survive the breakdown process could pollinate local populations, whereas small clumps and solitary pollen grains might be transported far enough to reach other populations. Lisci et al. (1996) suggested that more "compact" dispersal due to pollen clumping might be an efficient dispersal strategy for the anemophilous herb *Mercurialis annua*, which grows in groups of closely spaced conspecifics. Our study provides quantitative support for the prediction of Lisci et al. (1996). However, our model indicates that the pollen dispersal distribution should be more heavily weighted at large downwind distances than would be expected if pollen clumps remained intact without disaggregation, thereby increasing genetic connectivity within populations. Many species along the continuum of pollination syndromes potentially exploit this strategy, especially self-incompatible plants that grow in dense groups, like *A. artemisiifolia*.

Further work is necessary to validate our hypothesis that pollen clumping is a previously overlooked strategy for pollen dispersal in wind-pollinated plants. Capturing individual disaggregation events on video would be an extremely difficult task; numerical modeling may be the best way to further investigate the problem. Modeling particulate disaggregation is still an uncertain science that involves the nature of particle cohesion and turbulent stresses at the smallest scales of environmental fluid motion (Lisci et al., 1996; Andersson and Andersson, 2006). Using data on the distribution of clump sizes as they initially shed from the flower, it should be possible to construct a more complete model of clumped pollen dispersal by accounting for the break-up of pollen clumps. Although it may be possible to model this phenomenon using analytical solutions to mathematical equations as we present here, numerical simulation techniques such as large eddy simulation (Pope, 2000) would be more appropriate. A large eddy simulation of pollen dispersion has been recently developed and validated (Chamecki et al., 2009). Such a model could be used to simultaneously simulate the dispersion of several clump sizes connected by a clump break-up model (Hill and Ng, 1995). Further investigation combining a model of this sort and paternity testing may eventually elucidate which environmental factors generate differences between pollen dispersal and pollen gene flow in anemophily.

LITERATURE CITED

ABUL-FATIH, H. A., AND F. A. BAZZAZ. 1979. The biology of *Ambrosia trifida* L. I. influence of species removal on the organization of the plant community. *New Phytologist* 83: 813–816.

ACKERMAN, J. D. 2000. Abiotic pollen and pollination: Ecological, functional, and evolutionary perspectives. *Plant Systematics and Evolution* 222: 167–185.

ANDERSEN, S. T. 1970. The relative pollen productivity and pollen representation of North European trees, and correction factors for tree pollen spectra. *Geological Survey of Denmark, series II* 96: 1–99.

ANDERSSON, R., AND B. ANDERSSON. 2006. Modeling the breakup of fluid particles in turbulent flows. *American Institute of Chemical Engineers Journal* 52: 2031–2038.

BASS, D. J., V. DELPECH, J. BEARD, P. BASS, AND R. S. WALLS. 2000. Late summer and fall (March–May) pollen allergy and respiratory disease in Northern New South Wales, Australia. *Annals of Allergy, Asthma & Immunology* 85: 374–381.

BIANCHI, D. E., D. J. SCHWEMMIN, AND W. H. WAGNER. 1959. Pollen release in the common ragweed (*Ambrosia artemisiifolia*). *Botanical Gazette* 120: 235–243.

BRUSH, G. S. 1989. Rates and patterns of estuarine sediment accumulation. *Limnology and Oceanography* 34: 1235–1246.

CHAMECKI, M., C. MENEVEAU, AND M. B. PARLANGE. 2009. Large eddy simulation of pollen transport in the atmospheric boundary layer. *Journal of Aerosol Science* 40: 241–255.

CHAMECKI, M., R. VAN HOUT, C. MENEVEAU, AND M. B. PARLANGE. 2007. Concentration profiles of particles settling in the neutral and

stratified atmospheric boundary layer. *Boundary-Layer Meteorology* 125: 25–38.

CULLEY, T. M., S. G. WELLER, AND A. K. SAKAI. 2002. The evolution of wind pollination in angiosperms. *Trends in Ecology & Evolution* 17: 361–369.

CURTIS, J. D., AND N. R. LERSTEN. 1995. Anatomical aspects of pollen release from staminate flowers of *Ambrosia trifida* (Asteraceae). *International Journal of Plant Sciences* 165: 29–36.

DAVIS, M. B. 1976. Erosion rates and land use history in southern Michigan. *Environmental Conservation* 3: 139–147.

DI-GIOVANNI, F., P. G. KEVAN, AND M. E. NASR. 1995. The variability in settling velocities of some pollen and spores. *Grana* 34: 39–44.

DINGLE, A. N., G. C. GILL, W. H. WAGNER, AND E. W. HEWSON. 1959. The emission, dispersion, and deposition of ragweed pollen. *In* H. E. Landsberg and J. Van Mieghem [eds.], Advances in geophysics, vol. 6, 367–387. Academic Press, New York, New York, USA.

DOW, B. D., AND M. V. ASHLEY. 1998. Factors influencing male mating success in bur oak, *Quercus macrocarpa. New Forests* 15: 161–180.

DOWDING, P. 1987. Wind pollination mechanisms and aerobiology. *International Review of Cytology* 107: 421–437.

FAEGRI, K., AND L. VAN DER PIJL. 1966. The principles of pollination ecology. Pergamon Press, Oxford, UK.

FAISON, E. K., D. R. FOSTER, I. W. W. OSWALD, B. C. S. HANSEN, AND E. DOUGHTY. 2006. Early Holocene openlands in southern New England. *Ecology* 87: 2537–2547.

FRIEDMAN, J., AND S. C. H. BARRETT. 2008. High outcrossing in the annual colonizing species *Ambrosia artemisiifolia* (Asteraceae). *Annals of Botany* 101: 1303–1309.

GENTON, B. J., A. SHYKOFF, AND T. GIRAUD. 2005. High genetic diversity in French invasive populations of common ragweed, *Ambrosia artemisiifolia*, as a result of multiple sources of introduction. *Molecular Ecology* 14: 4275–4285.

GHAZOUL, J. 2005. Pollen and seed dispersal among dispersed plants. *Biological Reviews of the Cambridge Philosophical Society* 80: 413–443.

GLASS, L., AND W. R. TOBLER. 1971. Uniform distribution of objects in a homogeneous field: Cities on a plain. *Nature* 233: 67–68.

GODSON, W. L. 1957. The diffusion of particulate matter from an elevated source. *Archive für Meteorologie, Geophysik, und Bioklimatologie* A10: 305–327.

GRIMM, E. C. 2001. Trends and paleoecological problems in the vegetation and climate history of the northern great plains, U.S.A. *Biology and Environment*, *Proceedings of the Royal Irish Academy, B: Biological, Geological, and Chemical Science* 101B: 47–64.

HAMRICK, J. L. 2004. Response of forest trees to global environmental changes. *Forest Ecology and Management* 197: 323–335.

HARDER, L. D., AND S. D. JOHNSON. 2008. Function and evolution of aggregrated pollen in angiosperms. *International Journal of Plant Sciences* 169: 59–78.

HESSE, M. 1981. The fine structure of the exine in relation to the stickiness of angiosperm pollen. *Review of Palaeobotany and Palynology* 35: 81–92.

HILL, P. J., AND K. M. NG. 1995. New discretization procedure for the breakage equation. *American Institute of Chemical Engineers Journal.* 41: 1204–1216.

KAIMAL, J. C., AND J. J. FINNIGAN. 1994. Atmospheric boundary layer flows: Their structure and measurement. Oxford University Press, New York, New York, USA.

KEPLER, J. 2009. The six-cornered snowflake. Paul Dry Books, Philadelphia, Pennsylvania, USA.

KISS, L., AND I. BÉRES. 2006. Anthropogenic factors behind the recent population expansion of common ragweed (*Ambrosia artemisiifolia* L.) in eastern Europe: Is there a correlation with political transitions? *Journal of Biogeography* 33: 2156–2157.

KNAPP, E. E., M. A. GOEDDE, AND K. J. RICE. 2001. Pollen-limited reproduction in blue oak: Implications for wind pollination in fragmented populations. *Oecologia* 128: 48–55.

LAAIDI, M., K. LAAIDI, J.-P. BESANCENOT, AND M. THIBAUDON. 2003. Ragweed in France: An invasive plant and its allergenic pollen. *Annals of Allergy, Asthma & Immunology* 91: 195–201.

LINDER, H. P. 1998. Morphology and the evolution of wind pollination. *In* S. J. Owens and P. J. Rudall [eds.], Reproductive biology in systematics, conservation and economic botany, 123–125. Royal Botanic Gardens, Kew, UK.

LISCI, M., G. CARDINALI, AND E. PACINI. 1996. Pollen dispersal and role of pollenkitt in *Mercurialis annua* L. (Euphorbiaceae). *Flora* 191: 385–391.

LORENZO, C., M. MARCO, D. M. PAOLA, C. ALFONSO, O. MARZIA, AND O. SIMONE. 2006. Long distance transport of ragweed pollen as a potential cause of allergy in central Italy. *Annals of Allergy, Asthma & Immunology* 96: 86–91.

NAKANISHI, A., N. TOMARU, H. YOSHIMARU, T. MANABE, AND S. YAMAMOTO. 2009. Effects of seed- and pollen-mediated gene dispersal on genetic structure among *Quercus salicina* saplings. *Heredity* 102: 182–189.

NATHAN, R. 2006. Long-distance dispersal of plants. *Science* 313: 786–788.

NATHAN, R., G. G. KATUL, H. S. HORN, S. M. THOMAS, R. OREN, R. AVISSAR, S. W. PACALA, AND S. A. LEVIN. 2002. Mechanisms of long-distance dispersal of seeds by wind. *Nature* 418: 409–413.

NIKLAS, K. J., AND S. L. BUCHMANN. 1988. Aerobiology and pollen capture of orchard-grown *Pistacia vera* (Anacardiaceae). *American Journal of Botany* 75: 1813–1829.

O'CONNELL, L. M., A. MOSSELER, AND O. P. RAJORA. 2006. Impacts of forest fragmentation on the mating system and genetic diversity of white spruce (*Picea glauca*) at the landscape level. *Heredity* 97: 418–426.

OKUBO, A., AND S. A. LEVIN. 1989. A theoretical framework for data analysis of wind dispersal of seeds and pollen. *Ecology* 70: 329–338.

PACINI, E., AND G. G. FRANCHI. 1998. Pollen dispersal units, gynoecium, and pollination. *In* S. J. Owens and P. J. Rudall [eds.], Reproductive biology in systematics, conservation and economic botany, 183–195. Royal Botanic Gardens, Kew, UK.

PASQUILL, F., AND F. B. SMITH. 1983. Atmospheric diffusion. John Wiley, New York, New York, USA.

PAYNE, W. W. 1966. Notes on the ragweeds of South America with the description of two new species: *Ambrosia pannosa* and *A. parvifolia* (Compositae). *Brittonia* 18: 28–37.

PLAYER, G. 1979. Pollination and wind dispersal of pollen in *Arceuthobium. Ecological Monographs* 49: 73–87.

POPE, S. B. 2000. Turbulent flows. Cambridge University Press, Cambridge, UK.

RAYNOR, G. S., E. C. OGDEN, AND J. V. HAYES. 1970. Dispersion and deposition of ragweed pollen from experimental sources. *Journal of Applied Meteorology* 9: 885–895.

ROUNDS, W. 1955. Solutions of the two-dimensional diffusion equations. *Transactions of American Geophysical Union* 36: 395–405.

SERRA, T., J. COLOMER, AND X. CASAMITJANA. 1997. Aggregation and breakup of particles in a shear flow. *Journal of Colloid and Interface Science* 187: 466–473.

SORK, V. L., AND P. E. SMOUSE. 2006. Genetic analysis of landscape connectivity in tree populations. *Landscape Ecology* 21: 821–836.

STACH, A., M. SMITH, C. A. SKJOTH, AND J. BRANDT. 2007. Examining *Ambrosia* pollen episodes at Poznan (Poland) using back-trajectory analysis. *International Journal of Biometeorology* 51: 275–286.

TAUBER, H. 1977. Investigations of aerial pollen transport in a forested area. *Dansk Botanisk Arkiv* 32: 1–121.

TONSOR, S. J. 1985. Leptokurtic pollen-flow, non-leptokurtic gene-flow in a wind-pollinated herb, *Plantago lanceolata* L. *Oecologia* 67: 442–446.

WANG, L. P., A. S. WEXLER, AND Y. ZHOU. 2000. Statistical mechanical description and modelling of turbulent collision of inertial particles. *Journal of Fluid Mechanics* 415: 117–153.

WANG, S. Y., S. A. SPONGBERG, AND J. S. RUBENSTEIN. 1985. Ragweed in China. *Nature* 316: 386.

WHITEHEAD, D. R. 1969. Wind pollination in the angiosperms: Evolutionary and environmental considerations. *Evolution* 23: 28–35.

WODEHOUSE, R. P. 1971. Hayfever plants. Hafner Publishing, New York, New York, USA.

YOUNGE, K., C. CHRISTENSON, A. BOHARA, J. CRNKOVIC, AND P. SAULNIER. 2004. A model system for examining the radial distribution function. *American Journal of Physics* 72: 1247–1250.